frontiers in Environmental Chemistry

ORIGINAL RESEARCH
published: 14 June 2021
doi: 10.3389/fenvc.2021.693509

Characteristics and Mechanism of Pb^{2+} Adsorption From Aqueous Solution Onto Biochar Derived From Microalgae and Chitosan-Modified Microalgae

Weigang Liu, Kelin Li*, Xi Hu*, Xinjiang Hu, Ruibin Zhang and Qi Li*

School of Environmental Science and Engineering, Central South University of Forestry and Technology, Changsha, China

OPEN ACCESS

Edited by:
Ehsan Nazarzadeh Zare, Damghan University, Iran

Reviewed by:
Farhad Ahmadijokani, University of British Columbia Okanagan, Canada
Zari Fallah, University of Mazandaran, Iran

***Correspondence:**
Weigang Liu
793471984@qq.com
Kelin Li
csfuklli@163.com
Xi Hu
Liam.ho@live.cn

Specialty section:
This article was submitted to Sorption Technologies, a section of the journal Frontiers in Environmental Chemistry

Received: *11 April 2021*
Accepted: *31 May 2021*
Published: *14 June 2021*

Citation:
Liu W, Li K, Hu X, Hu X, Zhang R and Li Q (2021) Characteristics and Mechanism of Pb^{2+} Adsorption From Aqueous Solution Onto Biochar Derived From Microalgae and Chitosan-Modified Microalgae. Front. Environ. Chem. 2:693509. doi: 10.3389/fenvc.2021.693509

With increasing aquatic heavy metal pollution and eutrophication, using algae to prepare novel adsorbent materials for remediating heavy metal pollution has recently attracted research attention worldwide. However, microalgae biochar exhibits poor adsorption capacity in certain conditions, and little is known regarding microalgae biochar modification using chitosan. Chitosan has been previously used to directly modify microalgae biochar; however, in this study, chitosan is used to modify algae powder used to prepare biochar. Therefore, in this study, chitosan was used as a microalgae biochar modifier to enhance its applicability and adsorption capacity. Accordingly, two new types of microalgae biochars, chitosan-biochar (CTS-BC) and biochar-chitosan (BC-CTS), were developed as an adsorbent material using *Clostridium* and adding chitosan as a modifier at different stages of its preparation. These developed microalgae biochars were characterized using Brunauer–Emmett–Teller surface area,X-ray photoelectron spectroscopy, Fourier transform infrared spectroscopy, and scanning electron microscopy. The adsorption processes of these biochars can be well described by a pseudo-second-order kinetic model. Pb^{2+} was dominantly adsorbed by microalgal biochar through chemisorption. Following chitosan modification, several mino, cyano, and aromatic ring groups were attached onto the surface of the microalgal biochar. The Pb^{2+} adsorption capacity of the chitosan-modified biochar was better than that of the unmodified biochar. The maximum Pb^{2+} adsorption capacity of CTS-BC under acidic conditions (pH = 5) was 9.41 mg g^{-1}, whereas that of BC-CTS under alkaline conditions (pH = 9) was 9.94 mg g^{-1}, both were higher than that of unmodified microalgae biochar under similar conditions. CTS-BC and BC-CTS possessed excellent stability and reusability for Pb(II) adsorption, the adsorption efficiency still remained above 50% even after three cycles. This study demonstrated that adsorbent materials having a stronger heavy-metal adsorption capacity can be prepared by adding chitosan during different stages of the microalgae biochar preparation process.

Keywords: microalgae biochar, modification, adsorption, chitosan, Pb^{2+}

INTRODUCTION

With the rapid development of industrial activities,a large amount of wastewater containing heavy metals is discharged to the environment, which has resulted in a number of serious problems. Heavy metals discharged to the environment include Cr,Zn,Cd,Ni,Ti,Cu,Hg, and others (Salomons et al., 2012). These heavy metals cannot be removed completely during water treatment, leading to the presence of persistent,bio-accumulative, and toxic residues in aquatic ecosystems, thus increasing their detrimental effects on ecosystems and public health (Sun et al., 2019).

Among them, Pb poisoning can cause abdominal colic, hepatitis, peripheral neuritis, and toxic encephalitis (Hu et al., 2012). The presence of Pb(II) in aquatic ecosystems has become an important environmental concern worldwide (Ayoub et al., 2013). Several methods have been applied for the remediation of polluted wastewater, including adsorption, electrokinetic remediation, ultrafiltration,membranes, chemical precipitation, and reverse osmosis (Inyang et al., 2016). However, many of these methods have high operating costs and create disposal problems due to the generation of toxic sludge and are not suitable for large scale implementation (Bordoloi et al., 2017). Therefore, among these technologies, adsorption is the most widely used method because of its design and operation flexibility, efficiency, and feasibility in practice (Purkayastha et al., 2014). Consequently, it is very desirable to prepare a low-cost,high-efficiency,ecofriendly adsorbent for environmental applications, especially for the application of low-cost,natural-based materials as adsorbents.

Biochar (BC) is a pyrolytic carbon-based solid derived from the biomass pyrolysis process. The environmental stability,well-developed porosity, and biocompatibility of BC endow it with wide application potential in many fields (Morales et al., 2015). Therefore, BC has been demonstrated to be a low-cost and highly efficient adsorbent with great potential in the elimination of pollutants from aqueous solutions. Recently, researchers developed engineered microalgae biochar adsorbents. Microalgal cells have good adsorption capacity and are easy to obtain. Therefore, microalgae biochar has economic and adsorption potential (Zheng et al., 2017). As a new type of adsorption material, microalgae biochar is a porous, stable, and carbon-rich solid material, it is produced from microalgae through the pyrolysis process under oxygen-limited conditions (Alhashimi and Aktas., 2017; Chang et al., 2015; Heilmann et al., 2010). Nevertheless, raw microalgae biochar usually has a limited capacity to adsorb contaminants from aqueous solutions due to its low surface area (Johansson et al., 2016; Awad et al., 2017). Furthermore, microalgae biochar often needs a large amount of addition in use, which increases the overall cost (Bird et al., 2011; Liu et al., 2021; Wu et al., 2020). Therefore, it is essential for biochar to be modified to enhance its metal adsorption ability.

Accordingly, modification methods include chemical modification, physical modification, loading with mineral oxides, and magnetic modification (Rajapaksha et al., 2016). Similarly, as a low-cost natural-based material, chitosan (CTS) may be an effective candidate for microalgae biochar adsorbent modifier. Its considerable amount of free amine and hydroxyl groups endow CTS with excellent heavy-metal-ion adsorbent abilities and make it a promising modification reagent for the adsorbent material matrix. For example, with the application of raw CTS as a dispersing and soldering reagent, the affinities of biochar adsorbents to Cd(II) and Pb(II) ions can be improved significantly (Zhou et al., 2013; Sun et al., 2014). These chitosan modification methods improve the physical structure of the adsorbent, as well as increasing the electrons, functional groups, and adsorption sites (Mohanty et al., 2006).

However, little is known on the application of chitosan-modified microalgae biochar for the adsorption of heavy metals with only a few published studies on the topic (Nethaji et al., 2013). In this study, microalgal biochar was prepared from *closterium*. To obtain microalgae biochar with a stronger adsorption capacity, we prepared the chitosan-modified microalgae biochar *via closterium* powder application before and after pyrolysis. The Pb^{2+} adsorption capacities of the microalgae biochar and of two kinds of chitosan-modified microalgae biochar were compared. Scanning electron microscopy (SEM), Fourier transform infrared (FTIR) spectroscopy, and Brunauer–Emmett–Teller (BET) surface area were used to analyze the mechanism of Pb^{2+} adsorption by microalgae biochar in different conditions.

MATERIALS AND METHODS

Algae Species

Closterium sp. (fachb-61) was purchased from the Freshwater Algae Culture Collection at the Institute of Hydrobiology in Wuhan, China.

Primary Instruments

Ultraviolet visible spectrophotometer (UV2700, Unocal, Shanghai); High-speed centrifuge (t-ws, Xiangyi Centrifuge, Changsha); Graphite furnace atomic absorption spectropho tometer (ice-3500, Thermo Fisher Company, United States); Surface Area Porosity Analyzer (LRH-100-GB, Taihong, Shaoguan); Scanning electron microscopy (Zeiss Sigma500, Germany), Infrared spectrometer (Spotlight 400 of PerkinElmer, United States); Tube Furnace (MXGX/200-R, Weixing, Shanghai). Zeta potential analyzer (Malvern Zetasizer Nano ZS90, United Kingdom). X-ray photoelectron spectroscopy (XPS) (ESCALAB 250,Thermo-VG Scientific, United States).

Main Chemical Reagents

Chitosan (Yuanye Shanghai); AceticAcid (Jingke Wuhan); Lead standard solution (Zhongchang Wuhan).

Biochar Preparation

Preparation of the unmodified biochar

Clostridium was grown in MA culture medium (**Table 1**) culture medium at 25°C with a light intensity of 2500lx–3000lx and a light/dark photoperiod of 12 h:12 h to exponential phase. The *Clostridium* powder was washed, dried,smashed, and sieved through a 200-mesh screen before use. Then, the algae powder was pyrolyzed in a furnace at 500°C in a N_2 atmosphere for 2 h. The obtained biochar was named BC.

TABLE 1 | Formulation of MA.

Components	Consumption	Concentration
$Ca(NO_3)\cdot 4H_2O$	1 ml L^{-1}	5 g/100 mldH_2O
KNO_3	1 ml L^{-1}	10 g/100 mldH_2O
$NaNO_3$	1 ml L^{-1}	4 g/100 mldH_2O
Na_2SO_4	1 ml L^{-1}	4 g/100 mldH_2O
$Mgcl_2\cdot 6H_2O$	1 ml L^{-1}	5 g/100 mldH_2O
B-Na_2glycerophsphate$\cdot 5H_2O$	1 ml L^{-1}	10 g/100 mldH_2O
Na_2EDTA	1 ml L^{-1}	0.5 g/100 mldH_2O
$MnCl_2\cdot 4H_2O$	1 ml L^{-1}	0.5 g/100 mldH_2O
$ZnCl_2\cdot 7H_2O$	1 ml L^{-1}	0.05 g/100 mldH_2O
$NaMnO_4\cdot 2H_2O$	1 ml L^{-1}	0.08 g/100 mldH_2O
$FeCl_2\cdot 6H_2O$	1 ml L^{-1}	0.05 g/100 mldH_2O
$CoCl_2\cdot 6H_2O$	1 ml L^{-1}	0.5 g/100 mldH_2O
H_2BO_3	1 ml L^{-1}	2g/100 mldH_2O
Bicine	0.5 g L^{-1}	—

Preparation of the Chitosan-Modified Microalgae Biochar

First, 1 g of CTS was dissolved in 100 ml of 2% acetic acid and magnetically stirred for 60 min; then, it stood overnight to fully dissolve. Subsequently,a certain amount of algae powder was immersed into the chitosan solution and magnetically stirred for 2 h. The chitosan-algae powder was washed, dried,smashed, and sieved through a 200-mesh screen before use. Afterward, the chitosan-algae powder was pyrolyzed in a furnace at 500°C in a N_2 atmosphere for 2 h. The biochar obtained in this manner was named CTS-BC. We also mixed BC with chitosan solutions directly and magnetically stirred them for 2 h. After centrifugation and drying to a constant weight, the chitosan-modified microalgae biochar (BC-CTS) was obtained.

Effect of Initial Heavy Metal Ion Concentration on Pb^{2+} Adsorption

BC,CTS-BC, and BC-CTS were placed in water solutions with different Pb^{2+} concentrations (5.0, 10.0, 15.0, 20.0, and 25.0 mg L^{-1}) with a solid-to-liquid ratio of 0.1:50 (g:mL) at pH = 7. Samples were taken every 10 min, and high-speed centrifugation (rotating speed of 8,000 rpm for 2 min) was used to obtain the supernatant. The samples were filtered through a filter membrane (Whatman, 0.22 μm). This process was repeated three times and the average value was used as the Pb^{2+} concentration in the supernatant.

The calculation equation for the heavy-metal adsorption rate is as follows:

$$N = \frac{C1 - C2}{C1} * 100\% \quad (1)$$

N: Adsorption rate (%)

C_1: Heavy metal ion concentration in the water prior to adsorption (mg L^{-1}).

C_2: Heavy metal ion concentration in the water after adsorption (mg L^{-1}).

The equilibrium adsorption capacity equation is as follows:

$$Q_e = \frac{C_1 - C_2}{M} \times V \quad (2)$$

M: Adsorbent amount (g).

V: Volume of the solution to be measured (L).

Effect of Adsorbent Dosage on Pb^{2+} Adsorption

To examine the effect of adsorbent dosage on adsorption efficiency of Pb(II), The dosage of CTS-BC and BC-CTS were 0.05, 0.1, 0.15, 0.2 and 0.3 g, the initial concentration of Pb^{2+} solution was 20.0 mg L^{-1}, contact times 60min,pH = 3(CTS-BC), pH = 9(BC-CT). The remaining experimenting reaction conditions were similar as defined previously in *Effect of Initial Heavymetal Ion Concentration on Pb^{2+} Adsorption*.

Effect of Temperature on Pb^{2+} Adsorption

The influence of the reaction temperature on the Pb^{2+} adsorption of CTS-BC and BC-CTS was evaluated at 25, 35, 45, and 65°C.The CTS-BC and BC-CTS dosage were both 0.1 g, and the solid-liquid ratio was 0.1:50 (g:mL). The remaining experimental reaction conditions were similar as those defined in *Effect of Initial Heavymetal Ion Concentration on Pb^{2+} Adsorption*.

Effect of Initial pH of the Heavy Metal Ion Solutions on Pb^{2+} Adsorption

The impact of pH on Pb^{2+} adsorption was investigated by adjusting the initial Pb^{2+} solutions (20 mg L^{-1}). The solutions were adjusted to the desired pH values by adding negligible amounts of NaOH or HCl solution (g:mL). The pH was adjusted to 3, 5, 7, 9, and 11. The remaining experimental reaction conditions were similar as those defined in *Effect of Initial Heavymetal Ion Concentration on Pb^{2+} Adsorption*.

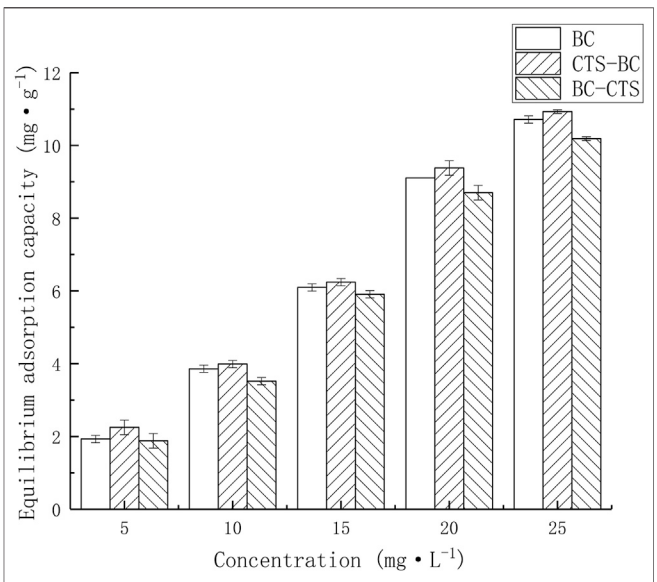

FIGURE 1 | Effect of initial concentration on Pb^{2+} adsorption.

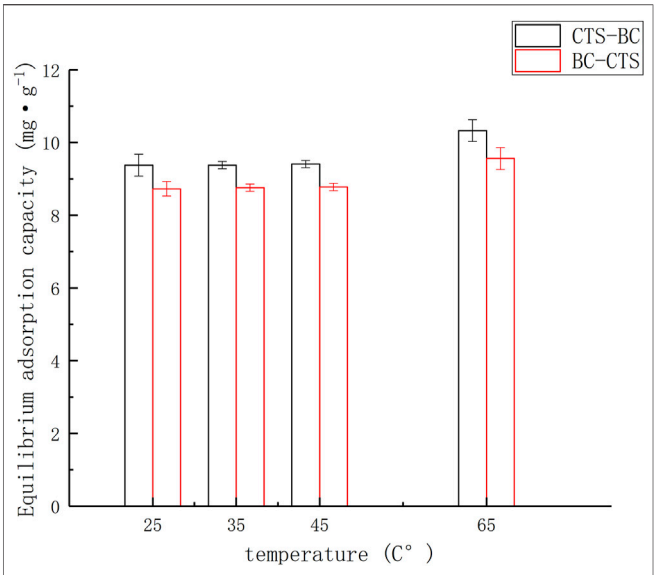

FIGURE 2 | Effect of reaction temperature on Pb^{2+} adsorption.

Desorption and Regeneration of Chitosan-Biochar and Biochar-Chitosan

The adsorption experimental reaction conditions were similar as those defined in *Effect of Initial Heavymetal Ion Concentration on Pb^{2+} Adsorption*. The adsorbed Pb^{2+} on CTS-BC and BC-CTS was desorbed by EDTA-NA_2 for 5 h in an oscillator at 200 rpm. For the regeneration analysis, the adsorption and desorption were conducted for three cycles.

Characterization of the Three Biochar Materials

All of the microalgae biochar were characterized with Fourier transform infrared (FTIR) spectroscopy,,Brunauer-Emmett-Teller Testing (BET) testing, scanning electron microscopy (SEM), and X-ray photoelectron spectroscopy (XPS) analysis methods. This was done to understand the surface characteristics and morphology and to analyze the relationship between the structural characteristics and adsorption performance of the adsorbents.

RESULTS AND DISCUSSION

Adsorption Performance and Kinetic Modeling

Adsorption Performance

The Pb^{2+} amount adsorbed onto the tested adsorbents [q_e = amount adsorbed per g of adsorbent at equilibrium (mg·g^{-1})] were plotted against initial Pb^{2+} concentrations [C_1 (mg L^{-1})], as shown in **Figure 1**. As the initial Pb^{2+} concentration increases, the equilibrium Pb^{2+} adsorption capacity of the three developed biochar materials also increases, which can be attributed to the existence of abundant active sites on the adsorbent surface. The adsorption capacity can continuous growth before saturation.

The Pb^{2+} amount adsorbed onto the tested adsorbents [q_e = amount adsorbed per g of adsorbent at equilibrium (mg·g-1)] were plotted against reaction temperature, as shown in **Figure 2**. The adsorption capacity of microalgae biochar to Pb^{2+} changed little at low temperature (25–45°C). The adsorption capacity of microalgae biochar to Pb^{2+} increased at 65°C, suggesting that the efficiency of microalgae biochar increases with increasing temperature.

The Pb^{2+} amount adsorbed onto the tested adsorbents [q_e = amount adsorbed per g of adsorbent at equilibrium (mg·g-1)] were plotted against adsorbent dosage, as shown in **Figure 3**. CTS-BC and BC-CTS showed similar regularity. As the adsorbent dosage increases, the adsorption rate increases, and the adsorption capacity decreases.

The results of three cycles of adsorption tests are presented in **Figure 4**. As shown in **Figure 4**, although the adsorption efficiency of Pb(II) on the regenerated CTS-BC and BC-CTS

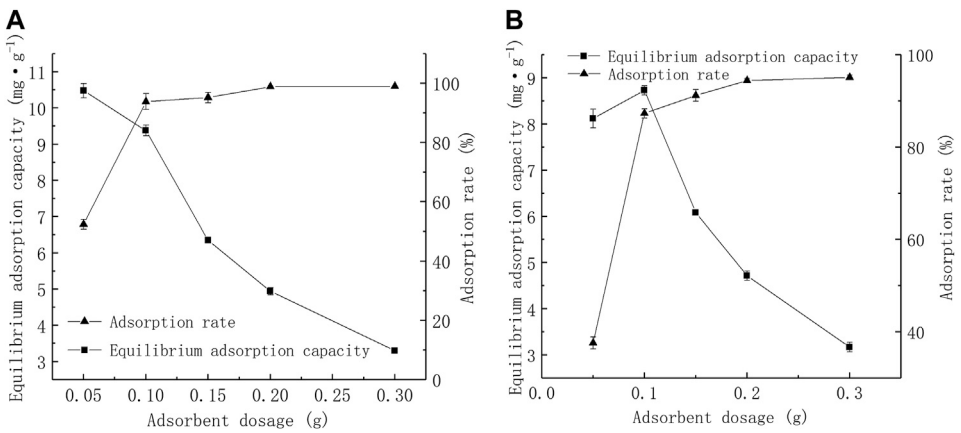

FIGURE 3 | Effect of dosage on Pb^{2+} adsorption.

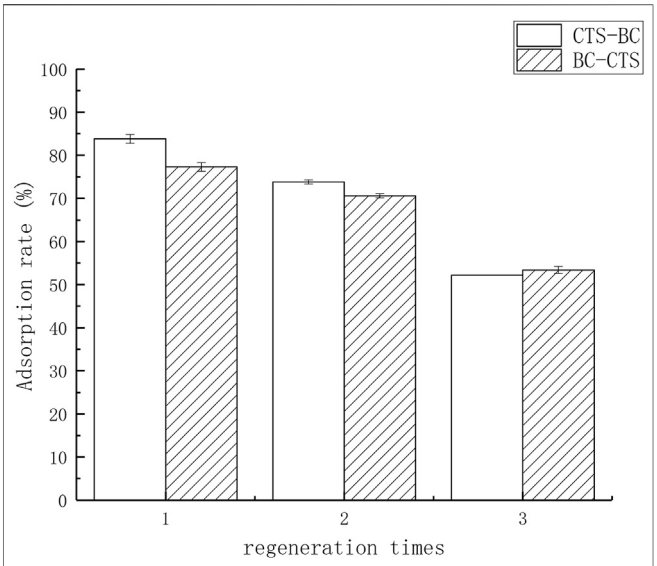

FIGURE 4 | Cyclic adsorption-desorption results.

slowly decreased with increasing cycle number, the adsorption efficiency still remained above 50% even after three cycles; this implied that CTS-BC and BC-CTS possessed excellent stability and reusability for Pb(II) adsorption. https://fanyi.baidu.com/?aldtype=16047 - ##https://fanyi.baidu.com/?aldtype=16047 - zh/en/javascript:void (0).

Adsorption Kinetics

The effect of contact time on Pb^{2+} adsorption is shown in **Figure 5**. All adsorbents exhibited fast Pb^{2+} adsorption during the initial 10 min, which was due to the sorption occurring at the surface, rather than in the micropores.

To elucidate on the adsorption mechanism, the adsorption capacity and rate tendencies were investigated using the pseudo-first-order and pseudo-second-order kinetic models. These microalgae biochar Pb^{2+} adsorption experiments were conducted under the condition of Pb^{2+} solutions (20.0 mg L^{-1}).

The linear form of two models can be presented as follows:

$$log\left(q_e - q_t\right) = logq_e - \frac{k_1}{2.303}t \tag{3}$$

$$\frac{t}{q_t} = \frac{1}{k_2 q_e^2} + \frac{1}{q_e}t \tag{4}$$

where q_t is the Pb^{2+} sorption amount (mg g^{-1}) at time t,q_e is the Pb^{2+} sorption.

Capacity at equilibrium (mg g^{-1}), and k_1 and k_2 are the pseudo-first-order and pseudo-second-order rate constants, respectively.

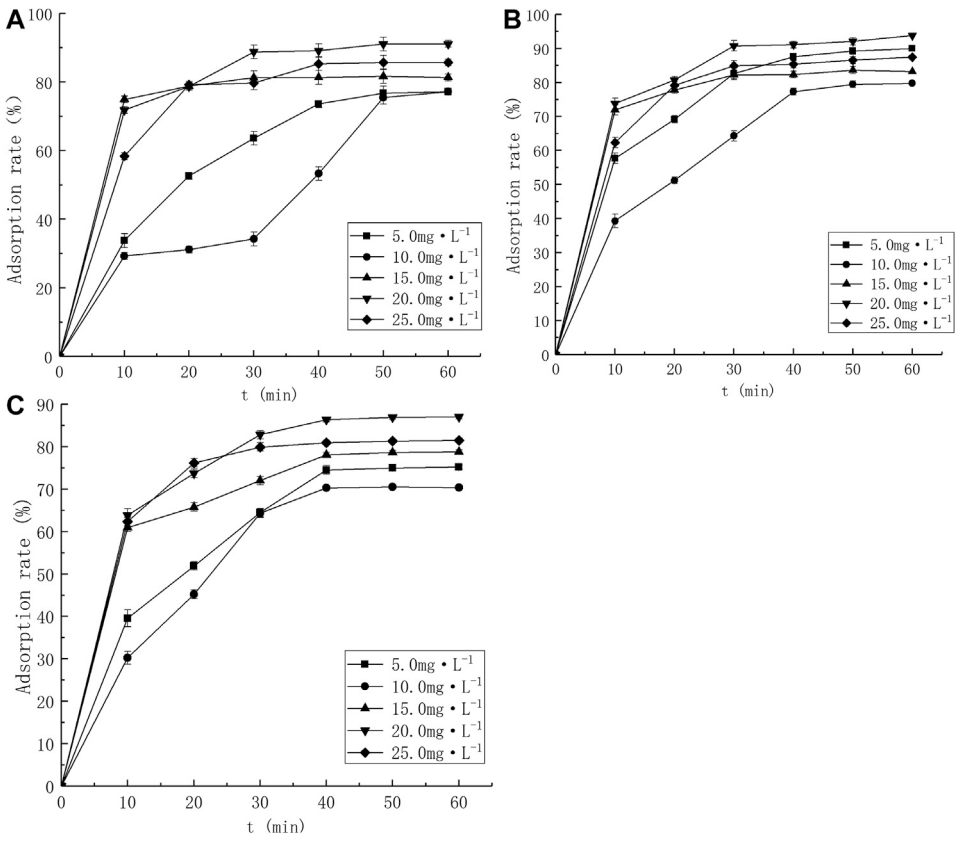

FIGURE 5 | Effect of reaction time on Pb^{2+} adsorption. **(A)**: BC,**(B)**: CTS-BC,**(C)**: BC-CTS.

TABLE 2 | Parameters for kinetics simulated by different equations.

	qe,exp (mg g^{-1})	Pseudo first-order kinetic model			Pseudo second-order kinetic model		
		qe, cal (mg g^{-1})	K_1	R^2	*qe, cal* (mg g^{-1})	K_2	R^2
BC	9.110	7.079	0.08	0.964	10.638	0.015	0.998
CTS-BC	9.380	3.631	0.064	0.912	9.958	0.026	0.999
BC-CTS	8.700	14.125	0.134	0.964	9.524	0.029	0.999

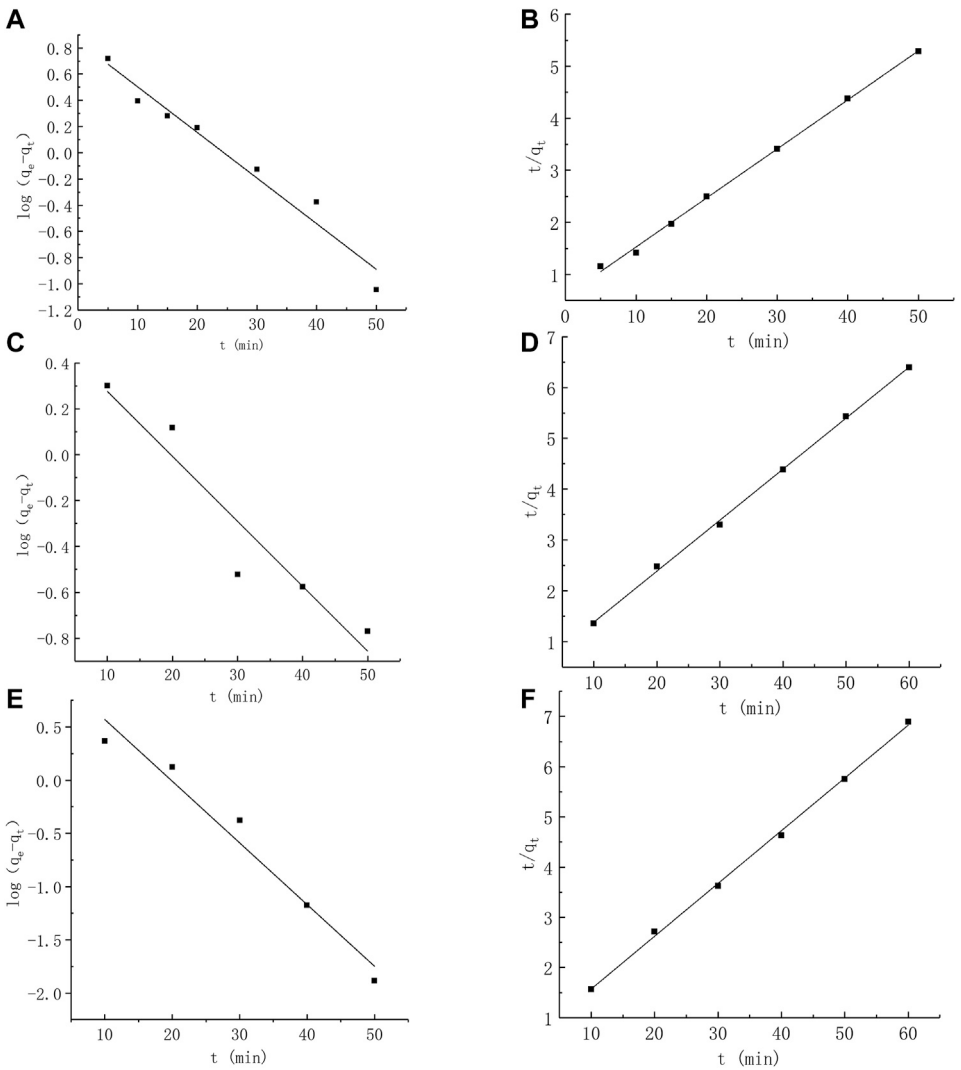

FIGURE 6 | Kinetic model of the adsorption on Pb^{2+} **(A)**: Pseudo first-order kinetic model of BC; **(B)** pseudo second-order kinetic model of BC; **(C)**: Pseudo first-order kinetic model of CTS-BC; **(D)** pseudo second-order kinetic model of CTS-BC; **(E)**: Pseudo first-order kinetic model of BC-CTS; **(F)** pseudo second-order kinetic model of BC-CTS.

The obtained analytical regression coefficients (R^2) and adsorption capacities are presented in **Table 2** and **Figure 6**. Pb^{2+} adsorptions onto BC,CTS-BC, and BC-CTS were best fitted by the pseudo-second-order model with $R^2 > 0.99$, and the calculated q_e values were nearly consistent with the experimental data. Therefore, the pseudo-second-order kinetic model fits for the adsorption process for all samples were considerably better than the pseudo-first-order model fits, suggesting that chemisorption is the governing factor that determines the Pb^{2+} adsorption.

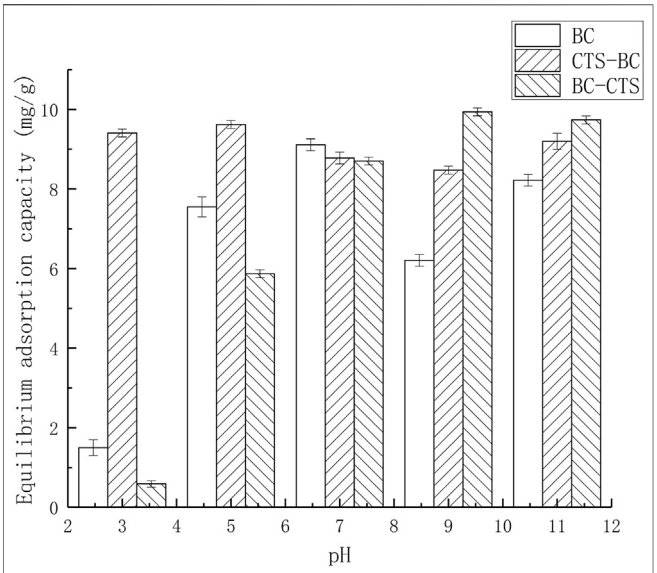

FIGURE 7 | Equilibrium adsorption capacity of the BC,CTS-BC, and BC-CTS under different pH conditions.

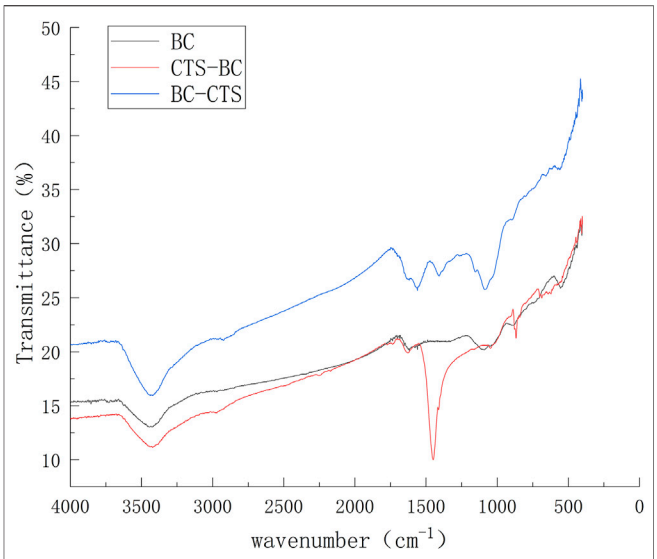

FIGURE 9 | Infrared spectra of the BC,CTS-BC, and BC-CTS before Pb^{2+} adsorption https://fanyi.baidu.com/?aldtype=16047–zh/en/javascript:void (0).

Effect and Comparison of Different Initial pH on the Adsorption of Pb^{2+} by Biochar, Chitosan-Biochar, and Biochar-Chitosan

The solution pH affected the surface charge of the adsorbent and the contaminant species because pH affects the metal-binding sites on the surface of the biochar adsorbents. However, the H^+ or OH^- ions present in the solution compete with Pb^{2+} for the adsorption sites on the biochar surface (Amin et al., 2018). The effects of the initial solution pH on the Pb^{2+} adsorption by BC,CTS-BC, and BC-CTS are illustrated in **Figure 7**.

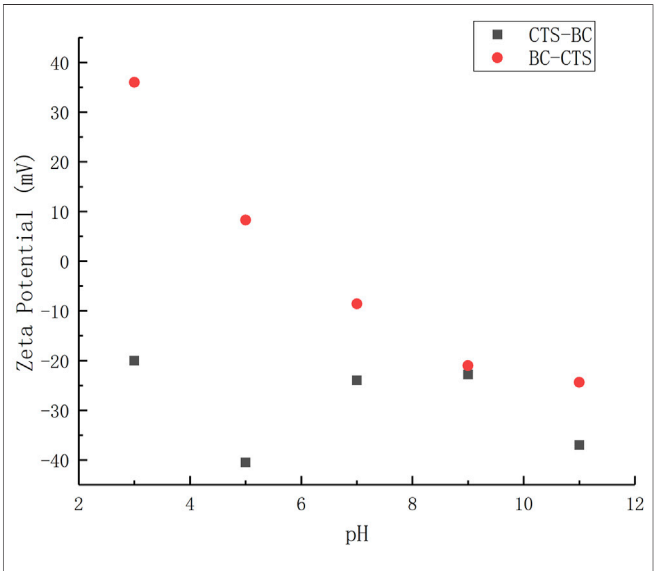

FIGURE 8 | Effect of solution pH on Zeta.

As shown in **Figure 7**, the Pb^{2+} adsorption capacities of the BC and BC-CTS adsorbents sharply decreased when the initial solution pH decreased from 7.00 to 3.00. This may be because under acidic conditions,H^+ ions in the aqueous solution combined with OH^- ions on the BC or BC-CTS surface and occupied the binding sites. A decrease in the solution pH was conducive to the surface protonation of adsorbent and resulted in the competition between H^+ and Pb^{2+}.However, the increasing pH gradually led to the change of positively charged adsorbent surface to negative because of the deprotonation effect. This resulted in increased electrostatic inductive interactions between the negatively charged surface and positive ions (Li et al., 2016). However,CTS-BC exhibited good adsorption performance under the same conditions, which may be due to the presence of numerous hydroxyl groups on the surface, which protect the adsorption sites. Therefore, the Pb^{2+} adsorption capacity of CTS-BC under acidic conditions was evidently better than that of BC.In addition, the Pb^{2+} adsorption capacity of BC-CTS under alkaline conditions was better than that of BC and CTS-BC. These results showed that CTS-BC was more suitable for acidic conditions, whereas BC-CTS was more suitable for alkaline environments. This may be because CTS-BC and BC-CTS are prepared through different methods, by adding chitosan during different stages of the biochar preparation process.

As shown in **Figure 8**, CTS-BC has a number of negatron under acidic conditions. therefore, the main mechanism was an electrostatic interaction at these pH values, electrostatic interactions may occur as a separate mechanism, which is the reason why CTS-BC has the stronger adsorption capacity under acidic conditions.

At low pH (3–5), the surface of BC-CTS was positively charged, This result suggests that electrostatic repulsion was present between BC-CTS and Pb^{2+}.That is why BC-CTS has

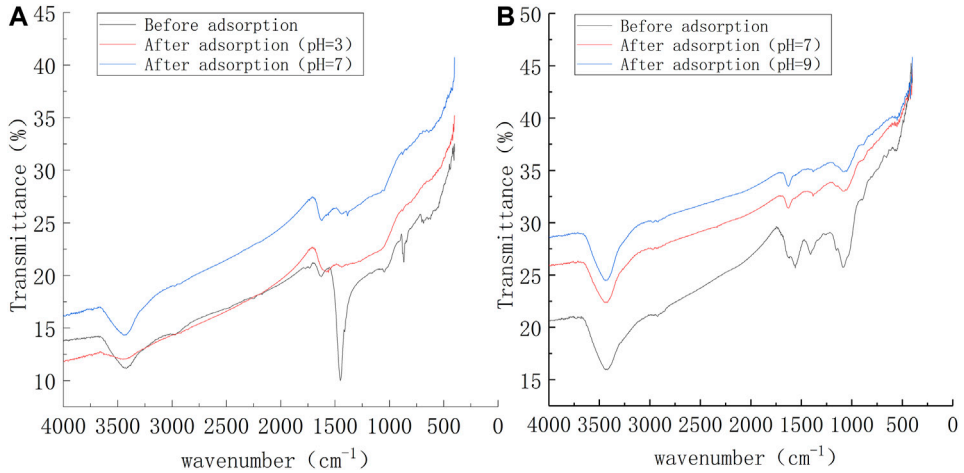

FIGURE 10 | Infrared spectra of the CTS-BC and BC-CTS after adsorption of Pb^{2+} under different conditions **(A)** CTS-BC and **(B)** BC-CTS.

weak adsorption capacity under acid condition. The positive charge of BC-CTS and the negative charge of Pb^{2+} at pH values between 6 and 11 allowed for electrostatic interactions that resulted in a higher Pb^{2+} adsorption capacity.

Biochar, Chitosan-Biochar, and Biochar-Chitosan Characterization

Specific Surface Area and Pore Size Analysis

Surface area and pore size are important properties of absorbing materials. The standard BET analysis results showed that the pore sizes of CTS-BC and BC-CTS are 23.550 and 12.773 nm (**Table 3**), both larger than that of BC. Although CTS-BC and BC-CTS had lower specific surface areas than BC, it had considerably higher Pb^{2+} adsorption, as revealed by the adsorption tests. These results suggest that microalgal biochar surface should have numerous functional groups functioning as active binding sites for Pb^{2+} adsorption. Therefore, we inferred that the microalgae biochar structure could be changed by adding chitosan at different stages of the preparation process.

Fourier Transform Infrared Spectroscopy

The functional groups responsible for Pb^{2+} adsorption on the microalgal biochar surface were determined through FTIR spectroscopy in the wavelength range of 4,000–500 cm^{-1}. As shown in **Figure 9**, BC,CTS-BC, and BC-CTS had conspicuous absorption bands at 3,443.95 cm^{-1}, and the typical peaks at 3,443.95 cm^{-1} can be attributed to O–H stretching vibrations. BC also had absorption peaks at 1,617.70 and 1,089.65 cm^{-1}, which can be attributed to aryl conjugated C=C and C–O stretching vibrations, respectively.Compared with BC, in the CTS-BC spectrum, new strong peaks were observed at 1,449.66 and 867.37 cm^{-1}. The adsorption observed at approximately 1,449.66 cm^{-1} can be attributed to N–N axial deformation in amino groups primarily due to chitosan Travlou et al. (2013), and the characteristic peak at 867.37 cm^{-1} can be ascribed to N–H bending vibration. With the further modification of BC with chitosan, the BC-CTS absorption peaks appeared at 1,560.72,1408.17, and 1,083.31 cm^{-1}, which may be attributed to the N–H inner bending vibration,C–O stretching vibration, and C–N stretching vibration, respectively (Huang et al., 2017). Compared with BC, there are more C–N and N–H vibrations on the CTS-BC and BC-CTS surfaces, respectively.These results confirm the efficient fabrication of CTS-BC and BC-CTS.

As shown in **Figure 10A**, two typical BC peaks observed at 1,449.66 and 867.37 cm^{-1} disappeared following Pb^{2+} adsorption, which indicated that during the Pb^{2+} adsorption by CTS-BC, the Pb^{2+} in the solution reacted with the N–N and N–H.Moreover, one shift of FTIR spectra was observed in CTS-BC before and after Pb^{2+} adsorption. The peak at 3,443.95 cm^{-1} was weakened, which indicate that the OH^- ions on the CTS-BC surface may have combined with H^+ ions in the solution. This is why CTS-BC can maintain its adsorption capacity, particularly under acidic conditions. As shown in **Figure 10B**, the BC-CTS peaks at 1,560.72,1408.17, and 1,083.31 cm^{-1} were weakened and shifted after Pb^{2+} adsorption, which indicated that amino,C–O, and cyano groups were the primary groups that affected the Pb^{2+} adsorption by BC-CTS. These results also confirm the efficient fabrication of CTS-BC and BC-CTS, indicating the feasibility of modifying microalgae biochar with chitosan.

TABLE 3 | Specific surface area and pore size analysis data of the three adsorbent materials.

Material	Specific surface area ($m^2 \cdot g^{-1}$)	Aperture (nm)
BC	3.922	3.415
CTS-BC	3.429	23.550
BC-CTS	3.755	12.773

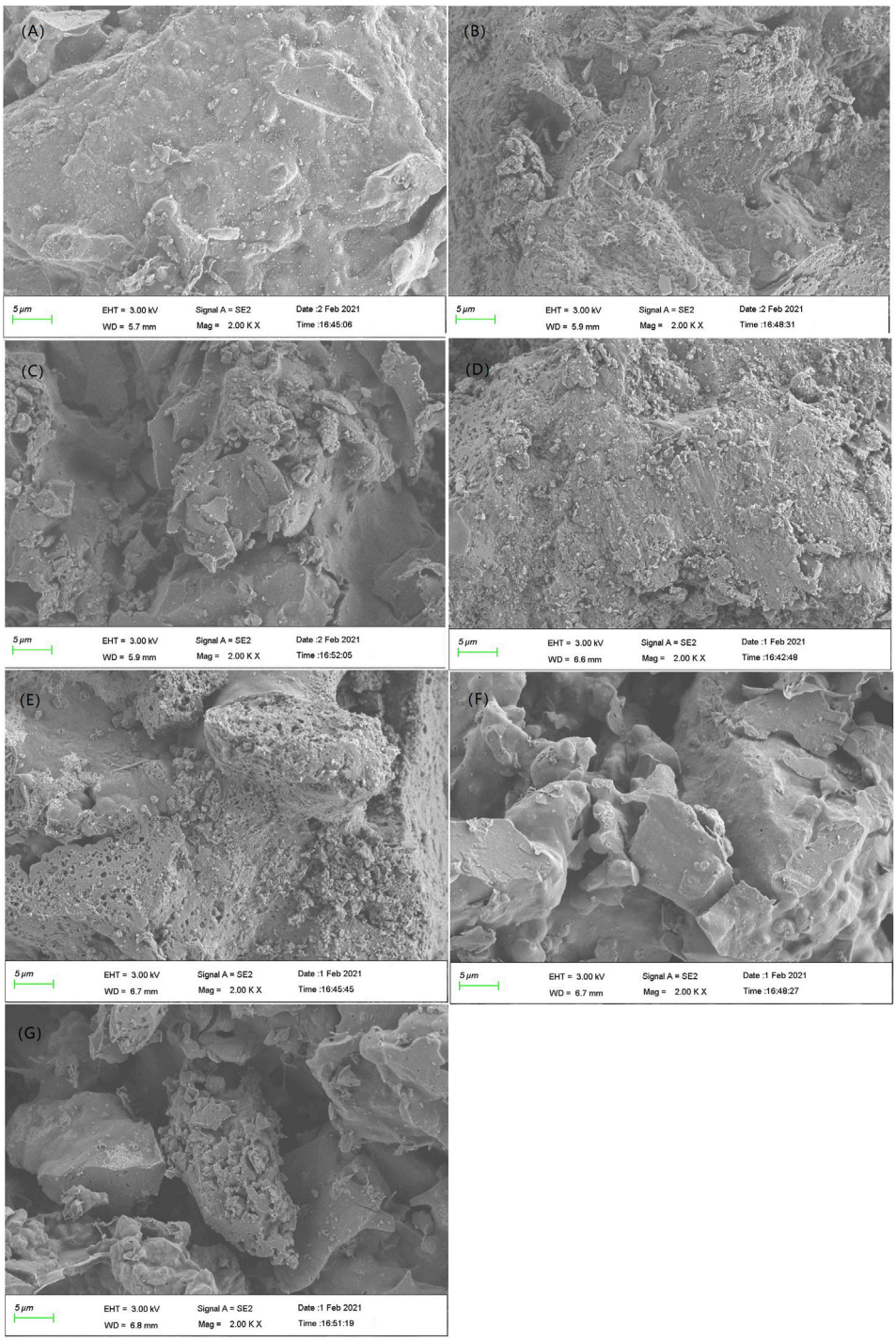

FIGURE 11 | SEM images of the three adsorbent materials.**(A)** BC without adsorption of Pb^{2+}; **(B)** CTS-BC without adsorption of Pb^{2+}; **(C)** BC-CTS without adsorption of Pb^{2+}; **(D)** adsorption of Pb^{2+} by the CTS-BC at pH = 3; **(E)** adsorption of Pb^{2+} by the CTS-BC at a pH = 7; **(F)** adsorption of Pb^{2+} by the BC-CTS at pH = 7; and **(G)** adsorption of Pb^{2+} by the BC-CTS at pH = 9.

Scanning Electron Microscope Characterization

The surface microstructure significantly affects the adsorption performance of an adsorbent (Amonette and Joseph., 2009; Elnour et al., 2019). Electron microscopy helps to observe the morphological changes of materials before and after the modification and adsorption. The BC,CTS-BC, and BC-CTS SEM images before and after Pb^{2+} adsorption are shown in **Figure 11**. The BC surface is relatively flat and smooth with

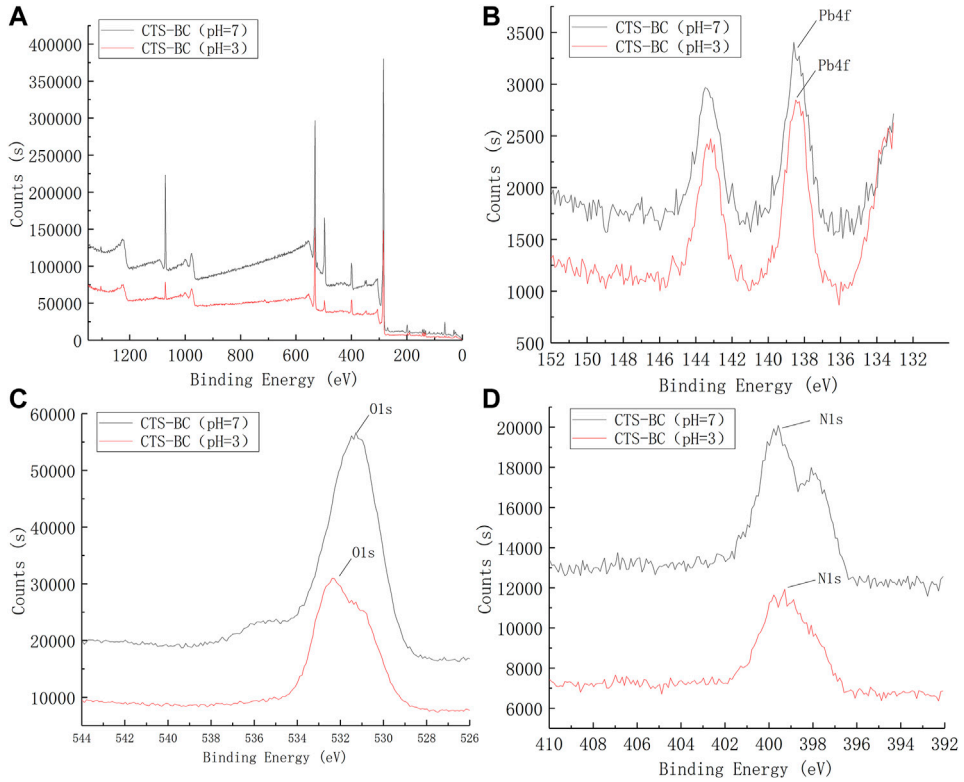

FIGURE 12 | XPS spectrum of CTS-BC. **(A)**:XPS wide scan of the CTS-BC, **(B)** Pb4f of CTS-BC, **(C)** O1s of CTS-BC, **(D)** N1s of CTS-BC.

the presence of small voids, as shown in **Figure 11A**. The CTS-BC SEM image before adsorption showed large voids and a rolling surface, whereas that after adsorption showed a smooth surface and a few bright spots (**Figures 11B,D**), which indicated that the Pb^{2+} on the surface of the post-sorption biochar filled the voids. Although there are numerous particles and micro holes on the surface after Pb^{2+} adsorption at pH = 7,CTS-BC still had a rolling surface (**Figures 11B,D,E**), which indicated that the CTS-BC surface will change under acidic conditions. Moreover, this is the reason for CTS-BC exhibiting more adsorption capacity under acidic conditions, as discussed in *Effect and Comparison of Different Initial pH on the Adsorption of* Pb^{2+} *by Biochar, Chitosan-Biochar, and Biochar-Chitosan*. The BC-CTS SEM image before adsorption exhibited sharp edges and corners, indicating that the chitosan was covered on the biochar surface (**Figure 11C**). Following Pb^{2+} adsorption, the BC-CTS surface was smooth and split (**Figures 11F,G**), which may be caused by van der Waals forces during Pb^{2+} adsorption.

X-Ray Photoelectron Spectroscopy Characterization

Next, the CTS-BC and BC-CTS samples after Pb^{2+} adsorption were also characterized through XPS analysis, as shown in **Figures 12**, **13**. Following Pb^{2+} adsorption, the CTS-BC and BC-CTS samples exhibited Pb3d XPS spectra, which indicated the presence of Pb^{2+} ions after adsorption. Based on the elemental analysis results presented in **Table 4**, the Pb content of CTS-BC at pH = 3 is 2.26%, which is higher than that of CTS-BC (0.06%) at pH = 9, thereby establishing that CTS-BC has good adsorption capacity under acidic conditions. Similarly, the Pb content of BC-CTS at pH = 11 is 0.09%, which is higher than that of BC-CTS at pH = 5, thereby establishing the good adsorption capacity of BC-CTS under alkaline conditions.

CONCLUSION

To improve the Pb^{2+} adsorption capacity of existing microalgae biochar, two novel chitosan-treated microalgae biochar (CTS-BC and BC-CTS) were developed, and their Pb^{2+} adsorption was tested.

The results presented herein revealed that CTS-BC and BC-CTS were effective adsorbents for Pb^{2+}、Zn^{2+} removal from aqueous solutions. The adsorption kinetics of the biochar were best described by the pseudo-second-order model. This apparently implies that chemisorption was the dominant Pb^{2+} adsorption process of microalgae biochar, which involves valence force through the sharing or exchange of electrons between adsorbate and adsorbent species. The adsorption capacity was affected by temperature and dosage. As the temperature and dosage increases, the equilibrium Pb^{2+} adsorption capacity of the three developed biochar materials also increases.

The Pb^{2+} adsorption capacity of BC was weakened under acidic and alkaline conditions. CTS-BC exhibited excellent Pb^{2+}

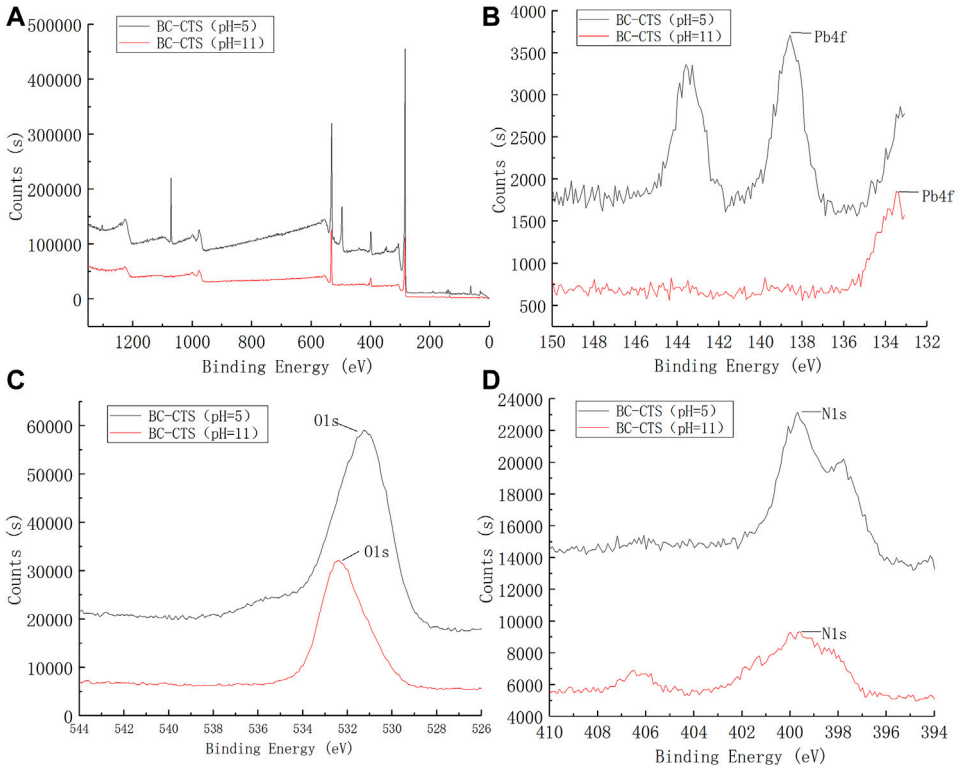

FIGURE 13 | XPS spectrum of BC-CTS. **(A)**:XPS wide scan of the BC-CTS, **(B)**Pb4f of BC-CTS, **(C)**O1s of BC-CTS, **(D)**N1s of BC-CTS.

TABLE 4 | Data of XPS.

	Element composition (%)			
	Pb	**N**	**O**	**C**
CTS-BC(pH = 9)	0.06	6.1	19.55	74.3
CTS-BC(pH = 3)	2.26	7.35	21.85	70.69
BC-CTS (pH = 5)	0.06	6.8	18.35	74.79
BC-CTS (pH = 11)	0.10	9.6	23.55	66.75

adsorption capacity under acidic conditions. The improvement of the CTS-BC adsorption capacity can be ascribed to the successful increase in the -OH,N–N, and N–H on the biochar surface. The maximum Pb^{2+} adsorption capacity at pH = 5 was 9.41 mg g^{-1}. However,BC-CTS exhibited excellent Pb^{2+} adsorption capacity under alkaline conditions. The improvement of the BC-CTS adsorption capacity can be attributed to the significant increase in the –OH,C–O,C–N, and N–H on the biochar surface. The maximum Pb^{2+} adsorption capacity at pH = 9 was 9.94 mg g^{-1}; however, it exhibited poor Pb^{2+} adsorption capacity under acidic conditions.

Therefore,CTS-BC is more suitable for acidic conditions (3 < pH < 7), whereas BC-CTS is more suitable for alkaline conditions (7 < pH < 11). Furthermore CTS-BC and BC-CTS possessed excellent stability and reusability for Pb(II) adsorption, the adsorption efficiency still remained above 50% even after three cycles.

DATA AVAILABILITY STATEMENT

The original contributions presented in the study are included in the article/Supplementary Material, further inquiries can be directed to the corresponding authors.

AUTHOR CONTRIBUTIONS

WL performed the main operation of the experiment experiment; RZ, and QL performed the preparation and assistance of experimental XiH, KL, and XinH helped perform the analysis with constructive discussions.

FUNDING

This work was financially supported by the Research and development projects of key fields in Hunan Province (Grant No. 2019SK2191), Natural Science Foundation of Hunan Province (Grant No. 2020JJ5984).

ACKNOWLEDGMENTS

We thank LetPub (www.letpub.com) for its linguistic assistance and scientific consultation during the preparation of this manuscript.

REFERENCES

Alhashimi, H. A., and Aktas, C. B. (2017). Life Cycle Environmental and Economic Performance of Biochar Compared with Activated Carbon: a Meta-Analysis. *Resour. Conservation Recycling* 118, 13–26. doi:10.1016/j.resconrec.2016.11.016

Amin, M. T., Alazba, A. A., and Shafiq, M. (2018). Removal of Copper and Lead Using Banana Biochar in Batch Adsorption Systems: Isotherms and Kinetic Studies. *Arab J. Sci. Eng.* 43 (11), 5711–5722. doi:10.1007/s13369-017-2934-z

Amonette, J. E., and Joseph, S. (2009). Characteristics of Biochar: Microchemical Properties. *Biochar Environ. Manag. Sci. Technol.* 33.

Awad, Y. M., Lee, S. E., Ahmed, M. B. M., Vu, N. T., Farooq, M., Kim, I. S., et al. (2017). Biochar, A Potential Hydroponic Growth Substrate, Enhances the Nutritional Status and Growth of Leafy Vegetables. *J. Clean. Produc.* 156, 581–588. doi:10.1016/j.jclepro.2017.04.070

Ayoub, A., Venditti, R. A., Pawlak, J. J., Salam, A., and Hubbe, M. A. (2013). Novel Hemicellulose-Chitosan Biosorbent for Water Desalination and Heavy Metal Removal. *ACS Sustainable Chem. Eng.* 1 (9), 1102–1109. doi:10.1021/sc300166m

Bird, M. I., Wurster, C. M., de Paula Silva, P. H., Bass, A. M., and De Nys, R. (2011). Algal Biochar - Production and Properties. *Bioresour. Technol.* 102 (2), 1886–1891. doi:10.1016/j.biortech.2010.07.106

Bordoloi, N., Goswami, R., Kumar, M., and Kataki, R. (2017). Biosorption of Co (II) from Aqueous Solution Using Algal Biochar: Kinetics and Isotherm Studies. *Bioresour. Technol.* 244, 1465–1469. doi:10.1016/j.biortech.2017.05.139

Chang, Y.-M., Tsai, W.-T., and Li, M.-H. (2015). Chemical Characterization of Char Derived from Slow Pyrolysis of Microalgal Residue. *J. Anal. Appl. pyrolysis* 111, 88–93. doi:10.1016/j.jaap.2014.12.004

Elnour, A. Y., Alghyamah, A. A., Shaikh, H. M., Poulose, A. M., Al-Zahrani, S. M., Anis, A., et al. (2019). Effect of Pyrolysis Temperature on Biochar Microstructural Evolution, Physicochemical Characteristics, and its Influence on Biochar/Polypropylene Composites. *Appl. Sci.* 9 (6), 1149. doi:10.3390/app9061149

Heilmann, S. M., Davis, H. T., Jader, L. R., Lefebvre, P. A., Sadowsky, M. J., Schendel, F. J., et al. (2010). Hydrothermal Carbonization of Microalgae. *Biomass and Bioenergy* 34 (6), 875–882. doi:10.1016/j.biombioe.2010.01.032

Hu, X., Zhang, Y., Ding, Z., Wang, T., Lian, H., Sun, Y., et al. (2012). Bioaccessibility and Health Risk of Arsenic and Heavy Metals (Cd, Co, Cr, Cu, Ni, Pb, Zn and Mn) in TSP and PM2.5 in Nanjing, China. *Atmos. Environ.* 57, 146–152. doi:10.1016/j.atmosenv.2012.04.056

Huang, B., Liu, Y., Li, B., Liu, S., Zeng, G., Zeng, Z., et al. (2017). Effect of Cu(II) Ions on the Enhancement of Tetracycline Adsorption by Fe3O4@SiO2-Chitosan/graphene Oxide Nanocomposite. *Carbohydr. Polym.* 157, 576–585. doi:10.1016/j.carbpol.2016.10.025

Inyang, M. I., Gao, B., Yao, Y., Xue, Y., Zimmerman, A., Mosa, A., et al. (2016). A Review of Biochar as a Low-Cost Adsorbent for Aqueous Heavy Metal Removal. *Crit. Rev. Environ. Sci. Technology* 46 (4), 406–433. doi:10.1080/10643389.2015.1096880

Johansson, C. L., Paul, N. A., De Nys, R., and Roberts, D. A. (2016). Simultaneous Biosorption of Selenium, Arsenic and Molybdenum with Modified Algal-Based Biochars. *J. Environ. Manage.* 165, 117–123. doi:10.1016/j.jenvman.2015.09.021

Li, M., Zhang, Z., Li, R., Wang, J. J., and Ali, A. (2016). Removal of Pb(II) and Cd(II) Ions from Aqueous Solution by Thiosemicarbazide Modified Chitosan. *Int. J. Biol. macromolecules* 86, 876–884. doi:10.1016/j.ijbiomac.2016.02.027

Liu, P., Rao, D., Zou, L., Teng, Y., and Yu, H. (2021). Capacity and Potential Mechanisms of Cd(II) Adsorption from Aqueous Solution by Blue Algae-Derived Biochars. *Sci. Total Environ.* 767, 145447. doi:10.1016/j.scitotenv.2021.145447

Mohanty, K., Jha, M., Meikap, B. C., and Biswas, M. N. (2006). Biosorption of Cr(VI) from Aqueous Solutions by *Eichhornia crassipes*. *Chem. Eng. J.* 117 (1), 71–77. doi:10.1016/j.cej.2005.11.018

Morales, V. L., Pérez-Reche, F. J., Hapca, S. M., Hanley, K. L., Lehmann, J., and Zhang, W. (2015). Reverse Engineering of Biochar. *Bioresour. Technol.* 183, 163–174. doi:10.1016/j.biortech.2015.02.043

Nethaji, S., Sivasamy, A., and Mandal, A. B. (2013). Preparation and Characterization of Corn Cob Activated Carbon Coated with Nano-Sized Magnetite Particles for the Removal of Cr(VI). *Bioresour. Technol.* 134, 94–100. doi:10.1016/j.biortech.2013.02.012

Purkayastha, D., Mishra, U., and Biswas, S. (2014). A Comprehensive Review on Cd(II) Removal from Aqueous Solution. *J. Water process Eng.* 2, 105–128. doi:10.1016/j.jwpe.2014.05.009

Rajapaksha, A. U., Chen, S. S., Tsang, D. C. W., Zhang, M., Vithanage, M., Mandal, S., et al. (2016). Engineered/designer Biochar for Contaminant Removal/immobilization from Soil and Water: Potential and Implication of Biochar Modification. *Chemosphere* 148, 276–291. doi:10.1016/j.chemosphere.2016.01.043

Sun, C., Chen, T., Huang, Q., Wang, J., Lu, S., and Yan, J. (2019). Enhanced Adsorption for Pb(II) and Cd(II) of Magnetic rice Husk Biochar by KMnO4 Modification. *Environ. Sci. Pollut. Res.* 26 (9), 8902–8913. doi:10.1007/s11356-019-04321-z

Sun, Y., Gao, B., Yao, Y., Fang, J., Zhang, M., Zhou, Y., et al. (2014). Effects of Feedstock Type, Production Method, and Pyrolysis Temperature on Biochar and Hydrochar Properties. *Chem. Eng. J.* 240, 574–578. doi:10.1016/j.cej.2013.10.081

Travlou, N. A., Kyzas, G. Z., Lazaridis, N. K., and Deliyanni, E. A. (2013). Functionalization of Graphite Oxide with Magnetic Chitosan for the Preparation of a Nanocomposite Dye Adsorbent. *Langmuir* 29 (5), 1657–1668. doi:10.1021/la304696y

W. Salomons, U. Förstner, and P. Mader (2012). *Heavy Metals: Problems and Solutions* (Springer Science Business Media).

Wu, P., Wang, Z., Wang, H., Bolan, N. S., Wang, Y., and Chen, W. (2020). Visualizing the Emerging Trends of Biochar Research and Applications in 2019: a Scientometric Analysis and Review. *Biochar* 2, 135–150. doi:10.1007/s42773-020-00055-1

Zheng, H., Guo, W., Li, S., Chen, Y., Wu, Q., Feng, X., et al. (2017). Adsorption of P-Nitrophenols (PNP) on Microalgal Biochar: Analysis of High Adsorption Capacity and Mechanism. *Bioresour. Technol.* 244, 1456–1464. doi:10.1016/j.biortech.2017.05.025

Zhou, Y., Gao, B., Zimmerman, A. R., Fang, J., Sun, Y., and Cao, X. (2013). Sorption of Heavy Metals on Chitosan-Modified Biochars and its Biological Effects. *Chem. Eng. J.* 231, 512–518. doi:10.1016/j.cej.2013.07.036

Conflict of Interest: The authors declare that the research was conducted in the absence of any commercial or financial relationships that could be construed as a potential conflict of interest.